applied sciences

MDPI

Article

The Assessment of the Technical Condition of Complex Fatigued Load-Carrying Structures

Robert Misiewicz * and **Jędrzej Stanisław Więckowski**

Faculty of Mechanical Engineering, Wroclaw University of Science and Technology, 50-370 Wrocław, Poland; Jedrzej.Wieckowski@pwr.edu.pl
* Correspondence: Robert.Misiewicz@pwr.edu.pl

Abstract: This article presents a research approach that enables the assessment of the technical condition of complex technical objects. The main emphasis is placed on the load-carrying structures of these objects. The procedure applying experimental research techniques and computer computations using the finite element method is described. The combination of the two techniques assesses the technical condition of the structure. The described approach is presented using the example of two objects.

Keywords: carrying structures; NDT; technical condition assessment

check for updates

Citation: Misiewicz, R.; Więckowski, J.S. The Assessment of the Technical Condition of Complex Fatigued Load-Carrying Structures. *Appl. Sci.* **2021**, *11*, 2449. https://doi.org/10.3390/app11062449

Academic Editor: Ricardo Branco

Received: 11 February 2021
Accepted: 3 March 2021
Published: 10 March 2021

1. Introduction

The issue of assessing the technical condition of industrial facilities is a problem that has been discussed in the academic community for years, where numerous approaches developed by scientists are implemented in industry [1–18]. There are many reasons for the need to assess the technical condition of machines. The two main reasons are operational safety and operational economic considerations. The first is often related to legal acts aimed at ensuring the safety of employees at workstations, and the second is an individual issue for each user entity.

Because of the ongoing global transformation, the economic aspect is more often connected with the ecological aspect. Increasing ecological demands require companies to modernize their production processes or completely change their business profile. Some branches of the extractive industries, which are characterized by a high initial investment cost and a long amortization time, are an example. New ecological trends and the related uncertainties regarding the prospects for further operation of some enterprises make the analysis of the profitability of replacing fatigued technical objects with new ones, for possibly a short service life, of extraordinary importance. A gradual economic transformation takes time. During this period, the plants must continue to function regularly, but the purchase of new facilities may be economically unprofitable. For these reasons, the aim is to use existing facilities for as long and as safely as possible. This requires periodic assessment of the technical condition based on which steps are taken to ensure the safety of their operation [19,20].

The assessment of technical condition is a complicated and time-consuming process; in the case of fatigued and old (often more than 20 years) load-carrying structures, it is additionally difficult. The reasons for complications include: the need to verify the current geometry of the object, considering numerous damages and structural changes that occurred during the operation period, and dealing with missing elements of technical documentation. The objects of investigation often operate in difficult conditions (dynamic loads, heat loads, and aggressive corrosion environments), making it challenging to carry out the verification [21–23].

Based on the assessment of the technical condition, a renovation policy is established, which extends the service life of the facilities. Such activities may lead to modernization; an example is the bucket wheel [12]. The methods of extending the service of technical objects include efficiency improvements [24], reduction in the dynamic loads' impact [25,26], and work safety improvements [27–29].

The following sections present the necessary steps to verify the technical condition of fatigued load-carrying structures. Each of the stages is described based on two different objects operating in a mineral processing plant. Such a plant is characterized by difficult operating conditions (destructive weather, chemical environment accelerating corrosion, and additional heat loads).

2. Step I—Inspection

The first stage in assessing the technical condition of a structure is conducting a visual inspection. The purpose of this stage is to detect structural deficiencies and identify areas that require further investigation.

The stage should be preceded by getting acquainted with the technical documentation of the structure to make researchers aware of the type and its specificity before the on-site visit. Knowledge of the operation history (failures, modernizations, etc.) also provides an important reference in assessing the technical condition. Then, the structure is inspected to identify any irregularities. These irregularities are:

(a) manufactural,
(b) operational, and
(c) mixed.

Manufactural irregularities are primarily related to deviations between the technical documentation and the state of the structure (Figure 1) [30]. Operational irregularities are linked to fatigue processes and manifest in the form of fatigue cracks (Figure 2) and plastic structure deformations (Figure 3). The mixed nature is associated with post-production and operational irregularities, where the observed defect may be the reason for both production or operation, but due to the long-term operations and ongoing fatigue processes, it is impossible to identify the source. These defects include: deficiencies and disintegration of structural joints (Figure 4), damage to the paint coating, and corrosion of the structure (Figure 5), as well as severe vibrations and displacements (Figure 6).

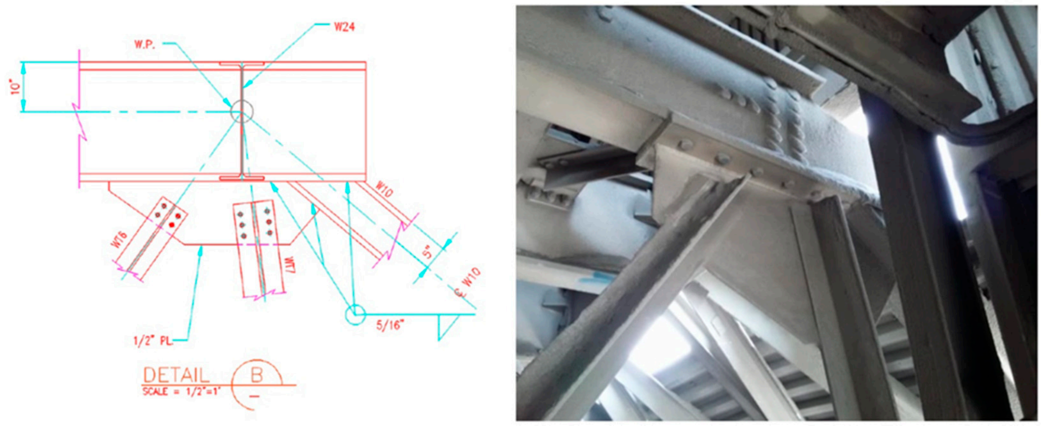

Figure 1. The shape of the gusset plate and the connection type (weld instead of bolts) do not match the documentation.

Figure 2. Fatigue cracks.

Figure 3. Plastics deformations.

Figure 4. Missing structural joints.

Figure 5. Damaged painting and corrosion centers.

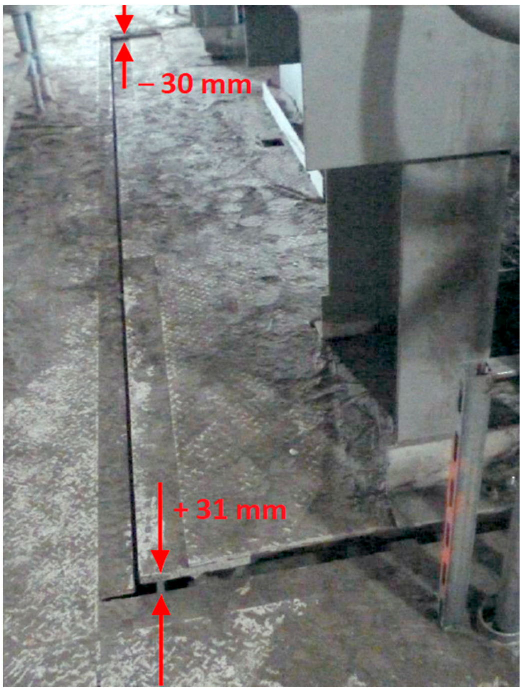

Figure 6. Displacements of the structure.

3. Step II—Technical Conditions Examination

The technical condition examination stage is crucial for the correctness of the technical condition assessment. At this stage, the key is to define the research area and the appropriate selection of measurement techniques [31–40]. Practice shows that for economic reasons, in-depth studies of all defects are not carried out and the research area is narrowed down to the most severe irregularities. The severity of the defects depends on how much they affect the current condition and further functioning of the structure and is related to the importance (places of occurrence) and the extent (number and size of occurrences) of the anomalies. When designating the area of research, a cause–effect analysis should be carried out to define the cause of the problems and their effects. The area of research should focus primarily on examining the causes of the problems to prevent them from arising in the future. Elimination of the effects is meaningful for the current state of the structure, while the elimination of the causes of problems is of key importance, as it determines its future state. The set of research and scope is an individual matter for each technical object. Examples of research for two diverse objects are presented in the following subsections.

3.1. Mineral Materials Processing Installation

The first example is mineral materials' processing cyclone installation. An inspection of the structure revealed several defects. Numerous corrosion centers, plastic deformations of the structure, cracks, and repairs were discovered. The working conditions and the type of damages determine the selection of measuring techniques. The presence of corrosion centers made it necessary to verify the current thickness of the elements of the structure and compare it with design thickness. This is important because as the cross-section area decreases, the stress level and buckling susceptibility increases. An ultrasonic thickness gauge was used for verification purposes (Figure 7). The thickness measurement results are presented in Figure 8. The measured values were compared with the design values and the percentage loss of the profile thickness is presented. Maximum losses reached as much as 36%, which posed a serious threat to the stability of the structure.

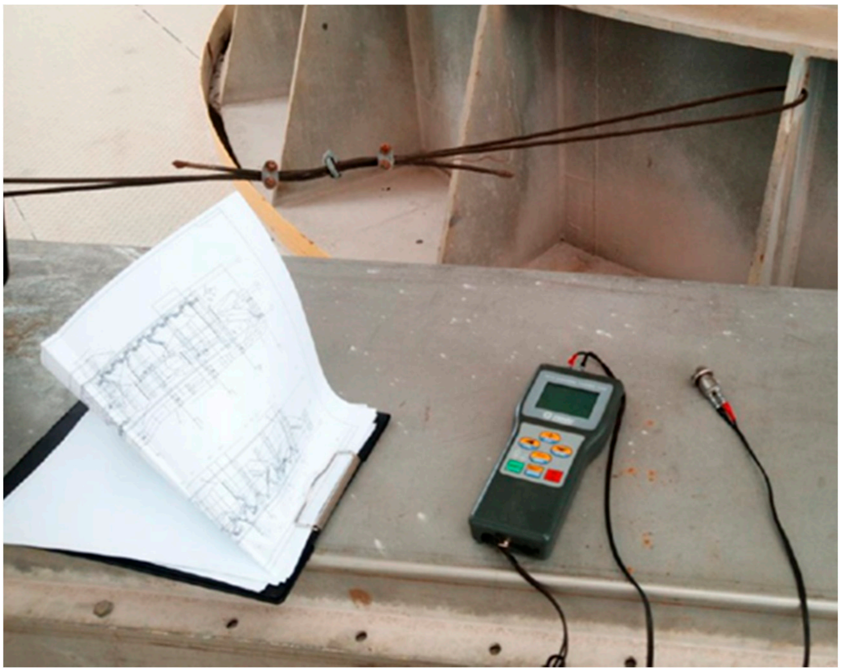

Figure 7. Ultrasonic thickness measurements.

The assessment of the technical condition of the object of investigation was necessary due to the numerous repairs already carried out. An example of such a process is shown in Figure 9. For years, renovation management involved local repairs, without looking for the causes of problems. Recurring defects made it necessary to perform a comprehensive assessment of the technical condition.

The structure, apart from numerous corrosion spots and cracks, suffered numerous plastic deformations. At the initial stage of the technical condition assessment, it was assumed that they were the result of buckling. Therefore, numerous thickness measurements were carried out (Figure 8). An example of the deformation is presented in Figure 10.

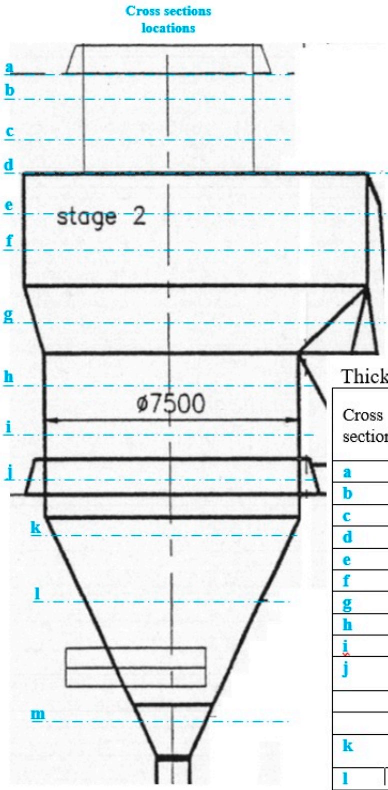

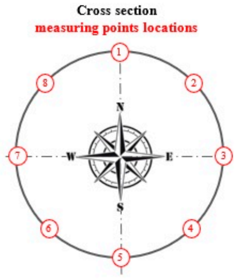

Thickness data

Cross section	Measuring points (see fig. above)									Original thickness*	REMARKS
	1	2	3	4	5	6	7	8	AVERAGE		
	CYCLONE PART										
a	4.6			5.5		5.4	5.7		**5.3**	6.0	
b	5.7	4.7	3.6	3.9	4.8	5.4	5.9	6.2	**5.0**	6.0	
c	5.1	2.1	4.3	3.4	5.1	5.6	5.7	4.9	**4.5**	6.0	
d	8.7	8.8	8.1	8.0	8.7	8.8	8.3	8.6	**8.5**	10.0	
e	7.3	7.8			7.5				**7.5**	8.0	
f	6.9	7.2							**7.1**	8.0	
g	6.4	7.1	5.9		7.3	7.4	7.1	6.5	**6.8**	8.0	
h	4.0	4.6	7.1	7.3	6.3	6.1	6.0	5.5	**5.9**	8.0	
i	6.2	6.3	5.6	4.9	6.9	5.1	4.5	7.1	**5.8**	8.0	
j	5.2	5.5	6.1	4.3	3.8	4.9	4.9	7.1	**5.2**	8.0	35% of thickness loss
AVERAGE THICKNESS LOSS									**19%**		
	CONE PART										
k	5.7	4.9	4.7	5.1					**5.1**	8.0	36% of thickness loss
l	4.8	5.6	6.1	6.5		6.3	4.8	4.8	**5.6**	8.0	
m	4.5	3.0	4.4	5.0		4.3	3.9	4.9	**4.3**	6.0	
AVERAGE THICKNESS LOSS									**32%**		

* - based on FLS thickness overview

Figure 8. Thickness measurements results of one of the segments.

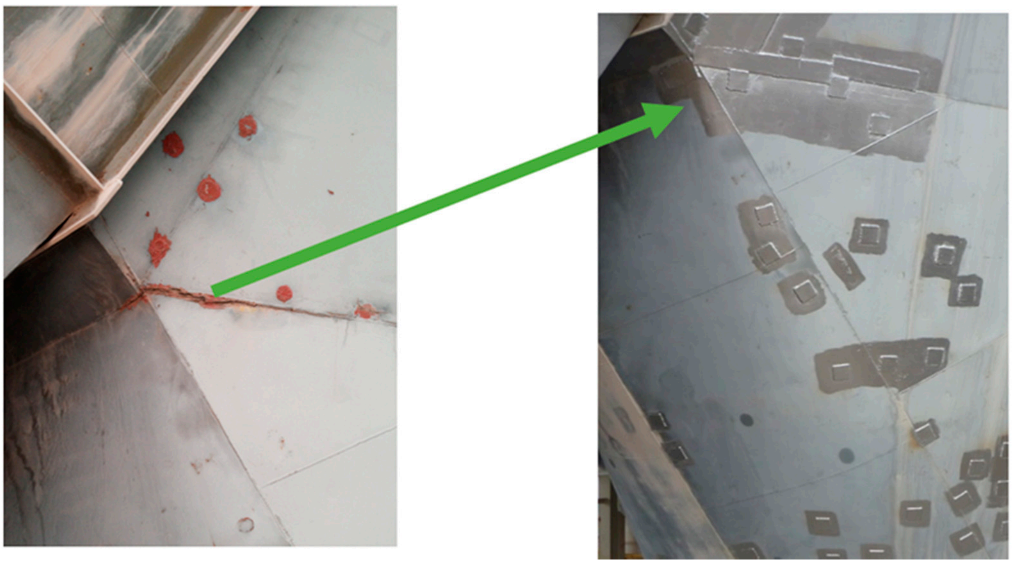

Figure 9. View of the structure before (**left side**) and after the repairs (**right side**).

Figure 10. Buckling deformation of the side wall.

Based on the study of technical documentation and operating conditions, the negative influence of the corrosive environment on the condition of the metal surfaces and thermal loads was assumed to be the cause of the problems. For this reason, a thermographic camera was used as a part of the technical condition measurements. The purpose was to acquire thermal operating conditions data and detect any internal damage to the insulating layer. Figure 11 presents a thermogram in which part of the insulation layer is damaged.

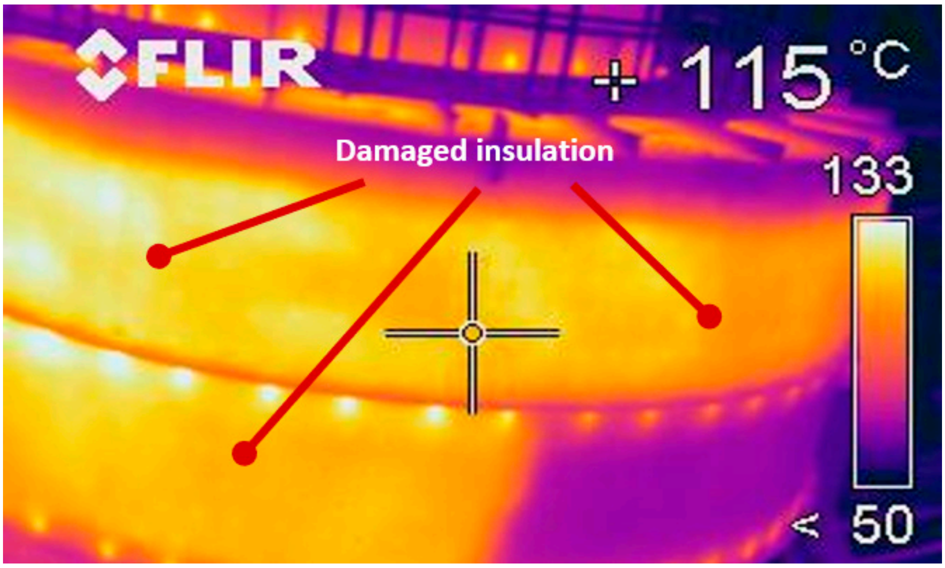

Figure 11. Thermogram of the damaged insulation layer region.

3.2. Loose Material Conveyor

The on-site inspection of the discussed object revealed many irregularities. These irregularities included defects in the form of numerous fatigue cracks, missing and disintegrations in structural joints, as well as deformations and severe vibrations of the structure. To check the degree of deformation, the structure was subjected to 3D scanning with the use of a laser scanner (Figure 12). The measurements confirmed the presence of anomalies in the geometry and allowed for their quantification. The top of the conveyor support was tilted 30 mm relative to the foundation (Figure 13).

Figure 12. 3D laser scanner.

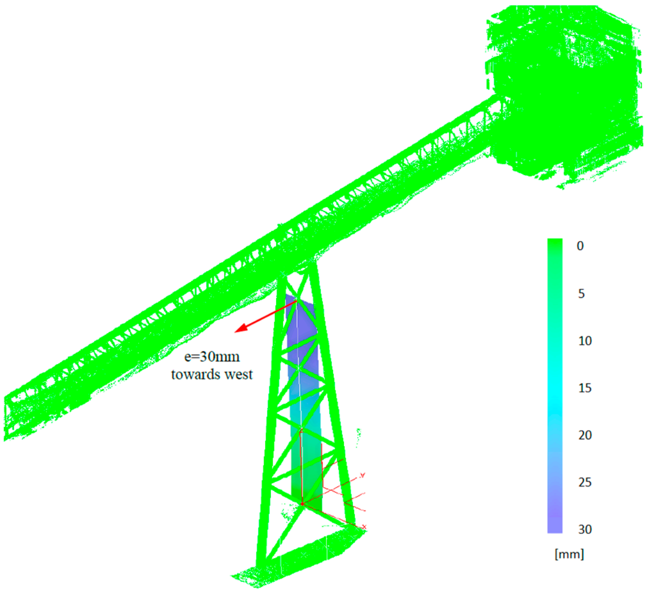

Figure 13. 3D scan of the structure.

Since strong vibrations of the structure were discovered during the local inspection, it was subjected to vibration measurements using acceleration sensors. Piezoelectric accelerometers (Figure 14) were used for the measurements. The conducted tests confirmed the occurrence of excessive vibrations. Due to the fast Fourier transform implementation, a significant amplitude of vibrations were detected for the frequencies 1.2, 3.9, and 9.0 Hz (Figure 15). These vibrations coincided with the excitation frequencies from the drive system, which potentially indicated that the structure operated in the frequency range of eigenfrequency. This led to resonance and a significantly accelerated rate of structure degradation that was manifested by the disintegration of the connections and the formation of fatigue cracks.

Figure 14. Vibration measurements.

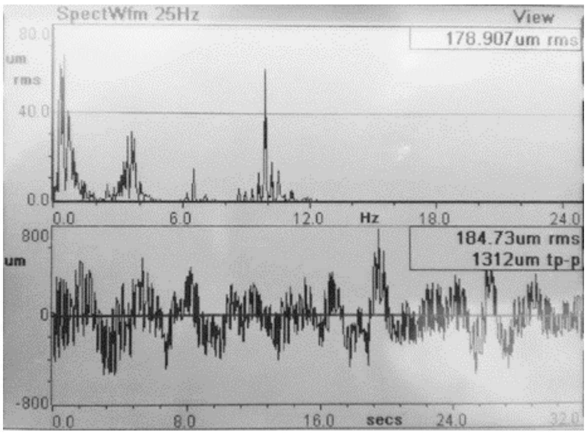

Figure 15. Amplitude–frequency spectrum of structure vibrations.

4. Step III—Technical Conditions Assessment

At this stage, it is necessary to verify the impact of the measured irregularities on the structure. This verification is usually based on computer-aided calculations [39,40]. In the case of the assessment of the technical condition of the load-carrying structures, the most-used calculation approach is based on the finite element method. This method is widely used for its versatility and the possibility of conducting various types of analysis as well as the relatively high accuracy of the results.

Considering the possibilities offered by computer-aided calculations, numerical calculations are the key stage in technical condition assessment. They make it possible to analyze the influence of the observed and measured defects on the condition of the structure. Based on the experimental research and the results of numerical analysis, the technical condition of the facility was assessed.

4.1. Finite Element Model Boundary Conditions

The use of numerical techniques allows determining the impact of the detected defects and non-conformities on the condition of the structure. However, to obtain representative results, appropriate boundary conditions consisting of the material model, constraints, and loads must be applied. The material model depends on the characteristics of the construction material and the type of analysis. Constraints depend on the foundation and fastening methods implemented in a structure, whereas loads depend primarily on the type of structure, its purpose, and specific operating conditions.

In the case of mineral materials processing installation, the structure was divided into two substructures: the first was responsible for material processing and the second for carrying the general loads and integrity. The structure's health issues were associated with the material processing part and it became the primary role of the investigation while the analysis of the second substructure was omitted. This approach provides valid results if the boundary conditions reflect the constraints of the object. This was achieved by applying the constraints to the material processing at the fastening spots within the second substructure. In the case of the conveyor, the whole structure was highly integrated and the approach could not be implemented. The finite model was constrained at the spots where the steel structure fastened to its foundations.

The selection of analysis type and loads application is an individual matter for a given structure and depends on whether or not it is subject to industrial regulations. In the case of structures that are subject to standards and legal regulations, instructions on the load conditions and analysis type can often be found in regulatory documents. If the analyzed structure is subject to this class of documentation, it is necessary to read them and apply any stated commands. In their absence, determining the load conditions and the type of analysis to be processed is an individual matter. The standards and regulations approach is correct when designing new objects and structures; however, it may not be suitable for fatigued ones. Structures facing health issues often suffer from factors (e.g., constant amplitude loads, random loads, heat loads, corrosion, etc.) that are not covered by regulation considerations, but still need to be identified and eliminated. This often requires out-of-the-box approaches resulting in an individual set of loads and analysis cases.

Considering the detected defects and the structures under investigation, individual sets of loads and analysis cases were established for each. In Tables 1 and 2, load and analysis cases are presented for materials processing installation and loose material conveyor, respectively.

Table 1. External forces included in the FEM (Finite Element Method) analysis—mineral materials processing installation.

Load Case (LC)	Loads				
	Dead, Live and Extraordinary Loads	**Dipping Tubes and Thimbles Weights**	**Under Pressure Loads**	**Temperature Loads**	**Storm Wind Loads**
Dead weight	+	+	−	+	−
LC1 horizontal wind	+	+	+	+	+
LC1 vertical wind	+	+	+	+	+
LC2	−	−	+	+	−

Table 2. External forces included in the FEM analysis—mineral materials processing installation.

Load Case	Loads					
	Dead Loads	**Active and Reactive Forces in the Conveyor Belt**	**Nominal Drive Torque**	**Peak Drive Torque**	**Displacement Load at the Conveyer Supporting Structure**	**Active and Reactive Forces, and Peak Drive Torque Considered as Constant Amplitude Time Variable, Gravity and Displacement Considered Static**
Drive system at nominal power	+	+	+	−	−	−
Drive system at overload	+	+	−	+	−	−
Displacement of the supporting mast	+	+	−	+	+	−
Modal Frequency Response	+	−	−	−	+	+

As part of the finite element method, simulations, boundary conditions, material models, and their properties should be defined. Generally, we can distinguish isotropic, anisotropic, and orthotropic material models and their behavior as linear elastic, nonlinear elastoplastic, or plastic. Choosing a representative material model and its behavior is vital for correct FEA (Finite Element Method) results and depends on both the material of which the structure is made and the type of analysis. In this research example, both structures were composed of S235 structural steel, with a minimum yield strength rated at 235 MPa. The specific characteristics of the material properties used in FEA are presented in Table 3. Since the macroscopic properties of steel alloys are generally considered isotropic and the FEA considerations of presented structures were within slight displacements of less than 5%, an isotropic linear elastic material model was implemented.

Table 3. Material properties used in FEA.

Material	Yield Strength (MPa)	Youngs Module (GPa)	Poisson's Ratio	Thermal Expansion Coefficient (μm/m·K)	Thermal Conductivity (W/m·K)
S235	235	210	0.3	12	42.5

An important aspect associated with finite element analysis is the interpretation of the results. It is particularly important in cases with multiaxial loading conditions and resulting multiaxial stresses, which were dealt with in the presented structures. For ductile materials, such as structural steel, the Huber–Mises stress theory identifies critical regions of the structure subjected to complex load conditions and compares the results directly to tensile yield stress, which enables the assessment of the safety margin of those regions. The presented stress distributions represent the stresses according to the Huber–Mises theory.

4.2. Mineral Materials Processing Installation

From the measurements of the identified irregularities alone, it was impossible to assess the condition of the structure. It was necessary to implement a verification method like a computer-aided finite element analysis. This method accounts for anomalies like local changes in the thickness of the structure elements, which diagnoses if a critical stress value has been exceeded. The results for the analysis of unfavorable operating conditions are presented in Figure 16. The FEA revealed that for the current thickness, the permissible stress value was exceeded. Detected areas should be urgently repaired as the probability of plastic deformation and/or fatigue cracks initiation, which may lead to failure, is exceptionally high. Another example of the use of numerical methods is considering the detected insulation issues that cause the formation of hotspots. The analysis accounts for the local temperature increase in the area where the insulating layer is damaged, which results in the formation of secondary thermal stresses and material weakening. The stress pattern for such a case is presented in Figure 17, where the analysis revealed the local exceeding of the permissible limit.

Numerical methods additionally allow for the performance of the buckling analysis. In the case of the examined structure, it was vital to verify whether the material thickness loss caused by the corrosion made the structure unstable and susceptible to buckling. The result of the buckling analysis is presented in Figure 18. The findings revealed that in the case of the most unfavorable operating conditions, the structure will buckle (buckling coefficient 0.71, calculated in the FEM analysis). The results concern the condition of the structure using the measured data acquired during the technical condition measurements.

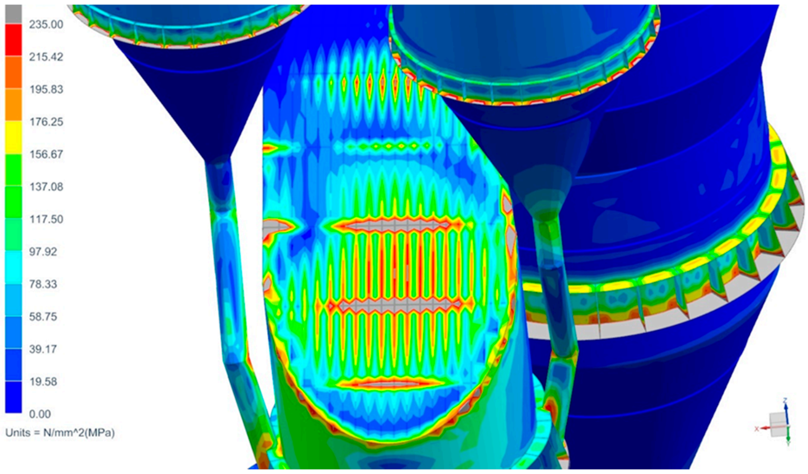

Figure 16. The stress pattern for the analysis accounting measured thickness, von Mises stresses MISSING.

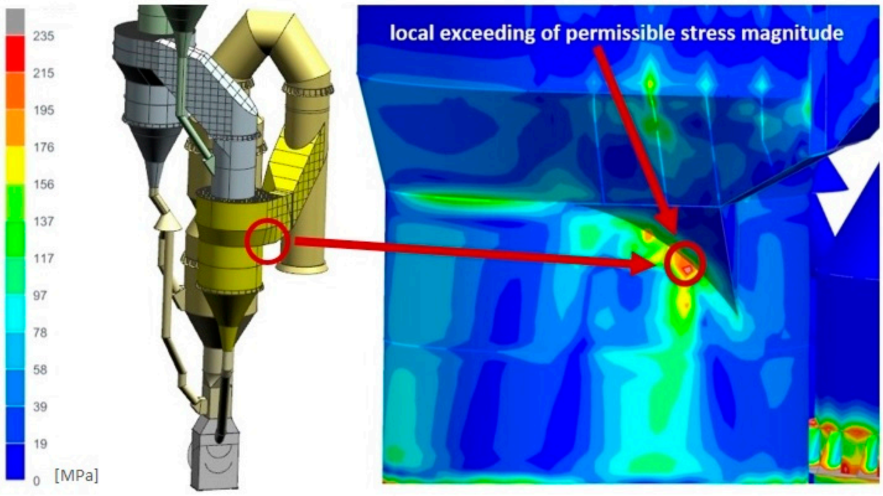

Figure 17. The stress pattern for the analysis accounting measured hotspots, von Mises stresses. The locations of this region is the area where the cylindrical part of the structure connects with the material transportation channel. At this place, the geometry changes significantly.

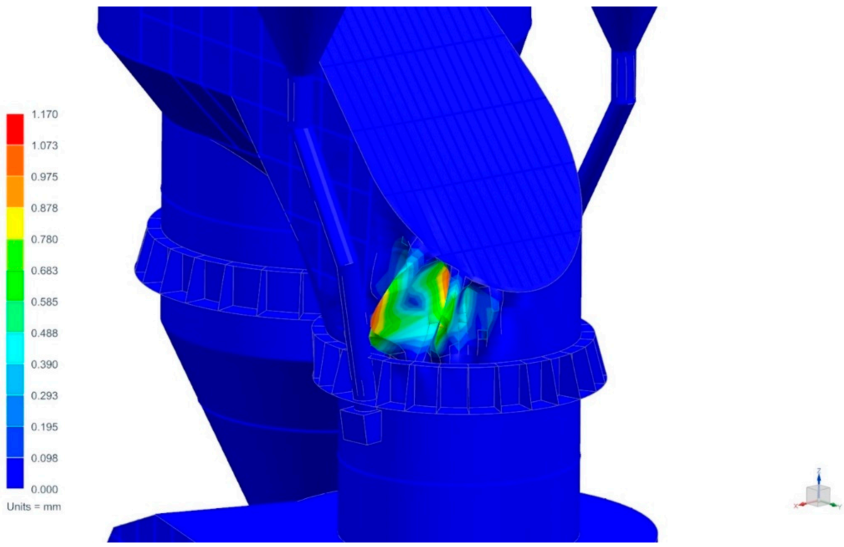

Figure 18. The global buckling mode of the structure.

4.3. Loose Material Conveyor

At the technical condition measurements stage, two important key irregularities were identified: deformations (Figure 6) and excessive vibrations of the structure. To check the causes of deformation, calculations were performed to check if it was possible to plasticize the structure, which is synonymous with its deformation, under the loads from the drive system with the conveyor operating at nominal power. Calculations showed this could not have happened. The further step in the analysis was to examine the structure's response to the loads caused by overloading the drive system. Overloading the structure did not cause observed deformation (Figure 6). Another attempt to detect the causes of deformation was the analysis of the influence of the displacement of the supporting mast structure on which the boom rests. 3D scanning revealed a discrepancy between the design and geometry of the supports (Figure 13). Considering the geometry of the supports in the numerical analysis caused the displacement of the structure in accordance with the measurement results (Figure 19).

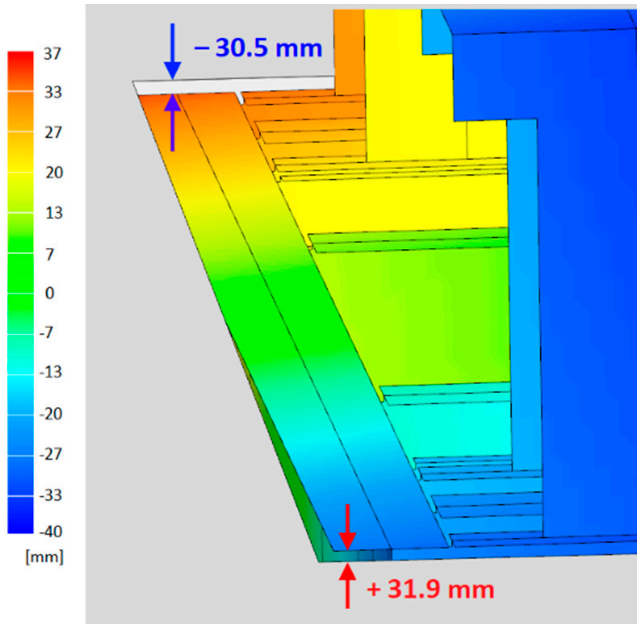

Figure 19. The structure displacements.

To determine the causes of the severe vibrations of the structure, which were the source of the fatigue cracks, joint disintegration, and an accelerated degradation rate, an analysis of the dynamic response of the structure subjected to the drive system loads was performed. Figure 21 presents the amplitude–frequency spectrum of the dynamic response of the structure. The colors of the curves represent the displacements at different points of the structure in the function of the load excitation frequency. These points are presented in Figure 20 (orange points along the conveyor boom). The Figure 21 analysis results showed a high vibration amplitude for frequencies 2.9, 9.2, 5.0, and 3.3 Hz, which are close to the measurement results. Calculations revealed that the structure worked under resonance frequency that caused high displacement magnitude, resulting in its premature wear. Figure 20 presents a 2.9 Hz vibration mode of the structure.

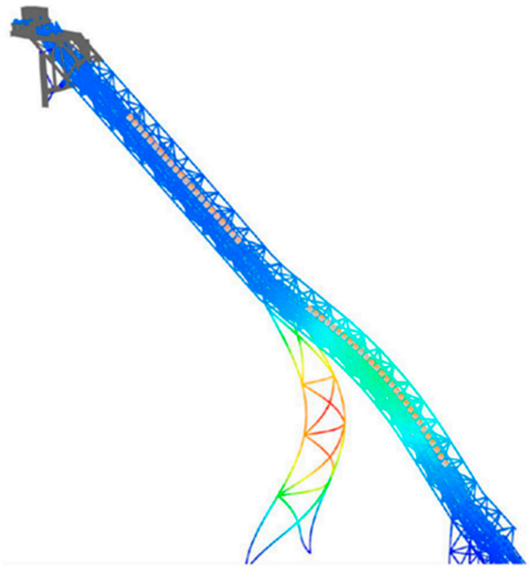

Figure 20. The 2.9 Hz vibration mode of the structure.

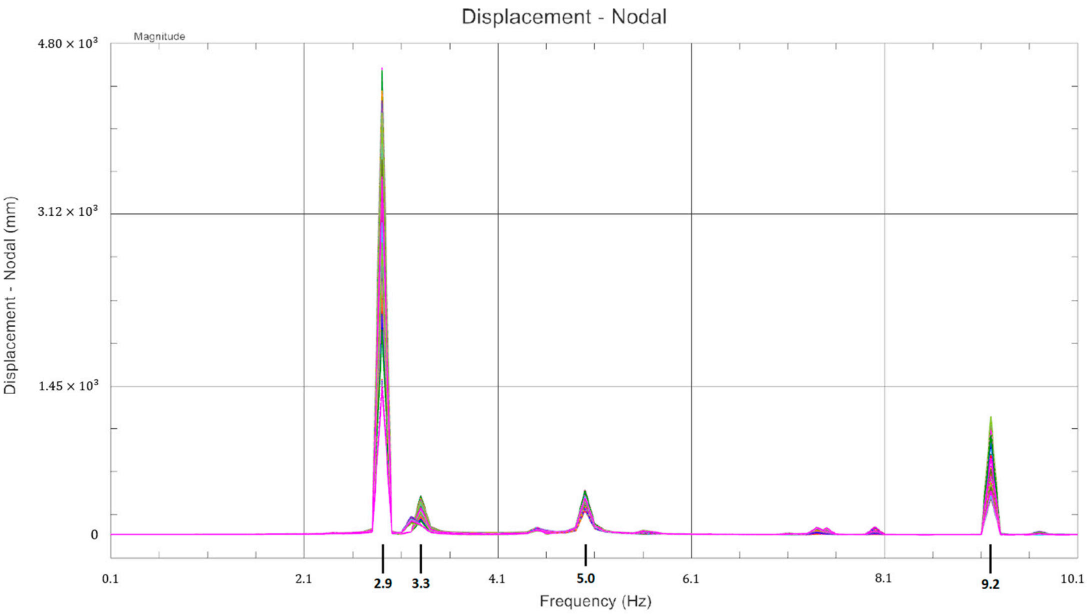

Figure 21. The amplitude–frequency spectrum of the dynamic response of the structure.

5. Summary and Conclusions

The paper presented the process of assessing the technical condition of two fatigued structures: the mineral materials processing installation and the loose material conveyor. There were significant differences between the objects regarding: their purpose (processing of materials, transporting), structure (thin-walled, frame), destructive factors (corrosion, vibrations), and the dominant symptoms of failure (buckling, fatigue cracks). Despite the differences, the process of assessing the technical condition consisted of the same steps of evaluation: preliminary visual inspection aimed at detecting irregularities, examining the technical condition quantifying the detected defects, and numerical calculations to establish their impact. These steps were necessary to assess the technical conditions of the structure.

In the case of the mineral materials installation, calculation of the linear statics and buckling was carried out, both considering thermal loads. The conveyor, linear static analysis accounting forces, and displacements loads were considered. The dynamic response of the system was also analyzed, and the amplitude–frequency vibration spectrum of the structure was established. Besides the differences in the measurement tools and analysis types implemented, the procedure was similar for both objects.

An important step in the assessment of the technical condition is the stage of numerical calculations, but it is crucial to consider the results of research conducted on real objects that are identified with the on-site visual inspection and technical conditions examination stages. This approach considers many design features of a tested object during numerical calculations, which would not be considered without the previous steps. As an example, local losses in the thickness of the material, local areas of increased temperature resulting from damage to the insulation layers, and design discrepancies compared with the technical documentation were considered. As a result, numerical calculations showed that regions with a high buckling potential (Figure 18) were possible to identify by considering the local irregularities in thickness found in the measurements and including them in the simulations.

The combination of presented procedures verified the level of operational safety of the structures and detected the dangers related to the further operation of the structures (e.g., buckling) before their occurrence. The results can be used to analyze various issues, for instance, selecting places that are exceptionally vulnerable to failure that should be subjected to constant monitoring and/or scheduling a maintenance policy. The economic assessment of the profitability of further exploitation is also a crucial issue and might be one of the key factors for industries that will have to undergo considerable transformation due to altering environmental regulations.

Author Contributions: Conceptualization, J.S.W.; methodology, R.M. and J.S.W.; formal analysis, R.M. and J.S.W.; investigation, R.M. and J.S.W.; writing: original draft preparation, R.M. and J.S.W.; writing: review and editing, R.M.; visualization, R.M. and J.S.W. All authors have read and agreed to the published version of the manuscript.

Funding: This research received no external funding.

Institutional Review Board Statement: Not applicable.

Informed Consent Statement: Not applicable.

Data Availability Statement: Not applicable.

Conflicts of Interest: The authors declare no conflict of interest.

References

1. Pietrusiak, D.; Smolnicki, T.; Stańco, M. The influence of superstructure vibrations on operational loads in the undercarriage of bulk material handling machine. *Arch. Civ. Mech. Eng.* **2017**, *17*, 855–862. [CrossRef]
2. Djurdjevic, D.; Maneski, T.; Milosevic-Mitic, V.; Andjelic, N.; Ignjatovic, D. Failure investigation and reparation of a crack on the boom of the bucket wheel excavator ERS 1250 Gacko. *Eng. Fail. Anal.* **2018**, *92*, 210–316. [CrossRef]
3. Arsić, D.; Gnjatović, N.; Sedmak, S.; Arsić, A.; Uhričik, M. Integrity assessment and determination of residual fatigue life of vital parts of bucket-wheel excavator operating under dynamic loads. *Eng. Fail. Anal.* **2019**, *105*, 182–195. [CrossRef]
4. Sakagami, T. Remote nondestructive evaluation technique using infrared thermography for fatigue cracks in steel bridges. *Fatigue Fract. Engng. Mater. Struct.* **2015**, *38*, 755–779. [CrossRef]
5. Cawley, P. Structural health monitoring: Closing the gap between research and industrial deployment. *Struct. Health Monit.* **2018**, *17*, 1225. [CrossRef]
6. Yu, Y.; Wang, C.; Gu, X.; Li, J. A novel deep learning-based method for damage identification of smart building structures. *Struct. Health Monit.* **2019**, *18*, 143. [CrossRef]
7. Ni, Y.Q.; Xia, Y.; Liao, W.Y.; Ko, J.M. Technology innovation in developing the structural health monitoring system for Guangzhou New TV Tower. *Struct. Control Health Monit.* **2009**, *16*, 73. [CrossRef]
8. Gibbs, B. Inspection Strategies. *Encycl. Marit. Offshore Eng.* **2017**, 1–12. [CrossRef]
9. Moczko, P.; Pietrusiak, D.; Rusiński, E. Material Handling and Mining Equipment—International Standards Recommendations for Design and Testing. *FME Trans.* **2018**, *46*, 291. [CrossRef]

10. Rusiński, E.; Stamboliska, Ż.; Moczko, P. Proactive control system of condition of low-speed cement machinery. *Autom. Constr.* **2013**, *31*, 313. [CrossRef]
11. Rusiński, E.; Moczko, P.; Odyjas, P.; Pietrusiak, D. Investigations of Structural Vibrations Problems of High Performance Machines. *FME Trans.* **2013**, *41*, 4.
12. Rusiński, E.; Cegiel, L.; Michalczyk, A.; Moczko, P.; Olejarz, J.; Pietrusiak, D. Investigation and modernization of buckets of surface mining machines. *Eng. Struct.* **2015**, *90*, 29. [CrossRef]
13. Awolusi, I.; Marks, E.; Hallowell, M. Wearable technology for personalized construction safety monitoring and trending: Review of applicable devices. *Autom. Constr.* **2018**, *85*, 96–106. [CrossRef]
14. Bossi, G.; Schenato, L.; Marcato, G. Structural Health Monitoring of a Road Tunnel Intersecting a Large and Active Landslide. *Appl. Sci.* **2017**, *7*, 1271. [CrossRef]
15. Farahani, B.; Barros, F.; Sousa, P.J.; Tavares, P.J.; Moreira, P.M.G.P. A railway tunnel structural monitoring methodology proposal for predictive maintenance. *Struct. Control Health Monit.* **2020**, *27*, e2587. [CrossRef]
16. Gkantou, M.; Rebelo, C.; Baniotopoulos, C. Life Cycle Assessment of Tall Onshore Hybrid Steel Wind Turbine Towers. *Energies* **2020**, *13*, 3950. [CrossRef]
17. De Oliveira, M.J.C.; Coelho, D.A. The integration of the standards systems of quality management, environmental management and occupational health and safety management. *Int. J. Prod. Res.* **2002**, *40*, 3857–3866. [CrossRef]
18. Viscardi, M.; Napolitano, P. ANN based approach to the structural health monitoring of a traction equipment. In Proceedings of the Recent Research in Electrical Engineering Conference, Lisbon, Portugal, 30 October–1 November 2014; Volume 11, pp. 189–198.
19. Lanzutti, A.; Magnan, M.; Maschio, S.; Fedrizzi, L. Failure analysis of a safety equipment exposed to EAF environment. *Eng. Fail. Anal.* **2019**, *95*, 107–116. [CrossRef]
20. Sanmiquel, L.; Bascompta, M.; Rossell, J.; Anticoi, H.; Guash, E. Analysis of Occupational Accidents in Underground and Surface Mining in Spain Using Data-Mining Techniques. *Int. J. Environ. Res. Public Health* **2018**, *15*, 462. [CrossRef] [PubMed]
21. Huo, L.; Li, C.; Jiang, T.; Li, H.-N. Feasibility Study of Steel Bar Corrosion Monitoring Using a Piezoceramic Transducer Enabled Time Reversal Method. *Appl. Sci.* **2018**, *8*, 2304. [CrossRef]
22. Moczko, P.; Pietrusiak, D.P.; Więckowski, J.S. Investigation of the failure of the bucket wheel excavator bridge conveyor. *Eng. Fail. Anal.* **2019**, *106*, 104180. [CrossRef]
23. Tang, J.; Li, J.; Wang, H.; Wang, Y.; Chen, G. In-Situ Monitoring and Analysis of the Pitting Corrosion of Carbon Steel by Acoustic Emission. *Appl. Sci.* **2019**, *9*, 706. [CrossRef]
24. Ono, K. Structural Health Monitoring of Large Structures Using Acoustic Emission—Case Histories. *Appl. Sci.* **2019**, *9*, 4602. [CrossRef]
25. Krazue, P.; Kasprzyk, J. Driving safety improved with control of magnetorheological dampers in vehicle suspension. *Appl. Sci.* **2020**, *10*, 8892. [CrossRef]
26. Krazue, P.; Kasprzyk, J.; Rzepecki, J. Experimental attenuation and evaluation of whole body vibration for an off-road vehicle with magnetorheological dampers. *J. Low Freqency Noise Vib. Act. Control* **2019**, *38*, 8542–8870. [CrossRef]
27. Baklouti, A.; Nguyen, N.; Mhenni, F.; Choley, J.-Y.; Mlika, A. Improved Safety Analysis Integration in a Systems Engineering Approach. *Appl. Sci.* **2019**, *9*, 1246. [CrossRef]
28. Gnjatović, N.B.; Bošnjak, S.M.; Milenović, I.L.; Stefanović, A.Z. Bucket wheel excavators: Dynamic response as a criterion for validation of the total number of buckets. *Eng. Struct.* **2020**, *225*, 111313. [CrossRef]
29. Rafajłowicz, W.; Więckowski, J.S.; Moczko, P.; Rafajłowicz, E. Iterative learning from suppressing vibrations in construction machinery using magnetorheological dampers. *Autom. Constr.* **2020**, *119*, 103326. [CrossRef]
30. Misiewicz, R.; Przybyłek, G.; Więckowski, J. Welding Procedure in Designing Carrying Structures of Machines. In *Proceedings of the 14th International Scientific Conference: Computer Aided Engineering*; Rusiński, E., Pietrusiak, D., Eds.; Springer: Cham, Switzerland, 2019; pp. 485–496. [CrossRef]
31. Sharpe, W.N. *Springer Handbook of Experimental Solid Mechanics*; Springer US: New York, NY, USA, 2008; ISBN 978-0-387-26883-5.
32. Civera, M.; Ferraris, M.; Ceravolo, R.; Surace, C.; Betti, R. The Teager-Kaiser Energy Cepstral Coefficients as an Effective Structural Health Monitoring Tool. *Appl. Sci.* **2019**, *9*, 5064. [CrossRef]
33. He, J.-H.; Liu, D.-P.; Chung, C.-H.; Huang, H.-H. Infrared Thermography Measurement for Vibration-Based Structural Health Monitoring in Low-Visibility Harsh Environments. *Sensors* **2020**, *20*, 7067. [CrossRef]
34. Lee, J.R.; Takatsubo, J.; Toyama, N.; Kang, D.H. Health monitoring of complex curved structures using an ultrasonic wavefield propagation imaging system. *Meas. Sci. Technol.* **2007**, *18*, 3816–3824. [CrossRef]
35. Wilde, K.; Miśkiewicz, M.; Chróścielewski, J. SHM System of the Roof Structure of Sports Arena "Olivia". In Proceedings of the 9th International Workshop On Structural Health Monitoring, Stanford, CA, USA, 10–12 September 2019; DEStech Publications, Inc.: Lancaster, PA, USA, 2013; pp. 1745–1752.
36. Sternini, S.; Quattrocchi, A.; Montanini, R.; di Scalea, F.L. Ultrasonic damage imaging of structural components with bulk and guided waves using match coefficients. In *Proceedings of the Health Monitoring of Structural and Biological Systems 2017*; Kundu, T., Ed.; SPIE: Washington, DC, USA, 2017; Volume 10170, p. 101701B.
37. Guidorzi, R.; Diversi, R.; Vincenzi, L.; Mazzotti, C.; Simioli, V. Structural monitoring of a tower by means of MEMS-based sensing and enhanced autoregressive models. *Eur. J. Control* **2014**, *20*, 4–13. [CrossRef]

38. Yang, M.; Qiao, P. Modeling and experimental detection of damage in various materials using the pulse-echo method and piezoelectric sensors/actuators. *Smart Mater. Struct.* **2005**, *14*, 1083–1100. [CrossRef]
39. Naranjo-Pérez, J.; Infantes, M.; Jiménez-Alonso, J.F.; Sáez, A. A collaborative machine learning-optimization algorithm to improve the finite element model updating of civil engineering structures. *Eng. Struct.* **2020**, *225*, 111327. [CrossRef]
40. Willberg, C.; Duczek, S.; Vivar-Perez, J.M.; Ahmad, Z.A.B. Simulation methods for guided wave-based structural health monitoring: A review. *Appl. Mech. Rev.* **2015**, *67*. [CrossRef]